Multi-depth photoacoustic microscopy with a focus tunable lens

Kiri Lee[a], Euiheon Chung[b], Tae Joong Eom[a*]

[a]Advanced Photonics Research Institute, Gwangju Institute of Science and Technology, Gwangju, 500-712, Republic of Korea

[b]Department of Medical System Engineering and School of Mechatronics, Gwangju Institute of Science and Technology, Gwangju, 500-712, Republic of Korea

*eomtj@gist.ac.kr

ABSTRACT

Optical-resolution photoacoustic microscopy (OR-PAM) has been studied to improve its imaging resolution and functional imaging modality without labeling on biology sample. However the use of high numerical aperture (NA) objective lens confines the field of view or the axial imaging range of OR-PAM. In order to obtain images at different layers, one needs to change either the sample position or the focusing position by mechanical scanning. This mechanical movement of the sample or the objective lens limits the scanning speed and the positioning precision. In this study, we propose a multi-depth PAM with a focus tunable lens. We electrically adjusted the focal length in the depth direction of the sample, and twice extended the axial imaging range up to 660 μm with the objective lens (20X, NA 0.4). The proposed approach can increase scanning speed and avoid step motor induced distortions during PA signal acquisitions without mechanical scanning in the depth direction. To investigate the performance of the multi-depth PAM system, we scanned a black human hair and the ear of a living nude mouse (BALB/c Nude). The obtained PAM images presented the volumetric rendering of black hair and the vasculature of the nude mouse.

Keywords: photoacoustic imaging, focus tunable lens, optical imaging, biomedical imaging

1. INTRODUCTION

Photoacoustic microscopy (PAM) has proved to be capable of noninvasive and functional biomedical imaging [1]. Based on the confocal configuration of optical illumination and acoustic detection, PAM can be classified into acoustic-resolution PAM (AR-PAM) and optical-resolution PAM (OR-PAM). OR-PAM systems provide high sensitivity to optical absorption contrast and have been studied to improve its imaging resolution and speed [2]. OR-PAM has been applied in many biomedical research fields, such as vasculature structure imaging [3-4]. However the axial imaging range of OR-PAM is limited by its short depth of focus due to a high numerical aperture (NA) objective lens. Various axial scanning methods have been implemented for laser scanning imaging systems to obtain volumetric images of biological tissue [5]. In previous study, the double-illumination PAM system was developed to improve the penetration depth and the expanded focal zone [6]. The double illumination PAM method need two different illumination beams on the top and bottom sides of an imaging sample. It requires additional bema splitting and focusing optical systems. To obtain images of different layers sequent, a high resolution optical imaging microscope system changes the sample position with the depth direction or the focusing depth position of an objective lens using translational stages or mechanical scanners [7-9]. This mechanical movement of the specimen or the objective lens limits scanning speed and the precision of the depth direction, and may be harmful to the sample. It could cause the risk of contact damage between the sample and objective lens. An optical beam-scanning method using an acoustic optic effect can enable relatively faster lateral scanning that is less susceptible to motion artifacts [10]. A focus tunable lens (FTL) has recently been applied in depth direction optical scanning on the three-dimensional optical tweezer [11] and the three-dimensional light-sheet microscopy [12].

Photons Plus Ultrasound: Imaging and Sensing 2015, edited by Alexander A. Oraevsky, Lihong V. Wang
Proc. of SPIE Vol. 9323, 93233O · © 2015 SPIE · CCC code: 1605-7422/15/$18
doi: 10.1117/12.2076709

In this study, we proposed a multi-depth laser beam illuminating method for a PAM system with a focus tunable lens. The proposed method electrically adjusted the focal length in the depth direction of the sample, and enhanced the axial imaging range. Furthermore, the proposed multi-depth PAM can increase scanning speed of the depth direction and avoid distortions during PA signal acquisitions without mechanical scanning with the depth direction.

2. MATERIALS AND METHODS

The schematic diagram of the multi-depth PAM system was depicted in Fig. 1(a). A diode pumped solid state pulsed laser (FQS-200-1-Y-532, Elforlight Ltd.) has 200 Hz pulse rate and 125 mW averaged output power at 532 nm wavelength. The Beam was expended to use fully aperture of objective lens and attenuated by neutral density filter. The attenuated beam was collimated by a convex lens. The collimated beam was focused by adjusting the focal length of an FTL. A tube lens was used to minimize the NA change in illumination on the sample [11]. Objective lens (20X, NA 0.4 and 50X NA 0.5) was used to obtain different axial imaging range. The proposed multi-depth PAM system consisted of the FTL (EL-10-30-C, Optotune Inc.) to control the focal position in axial scanning. The FTL is based on a local change of the refractive index of the composed material. The focal length of the FTL can be adjusted from 80 mm to 200 mm as changing the driving current, and the maximum response time is 2.5 msec.

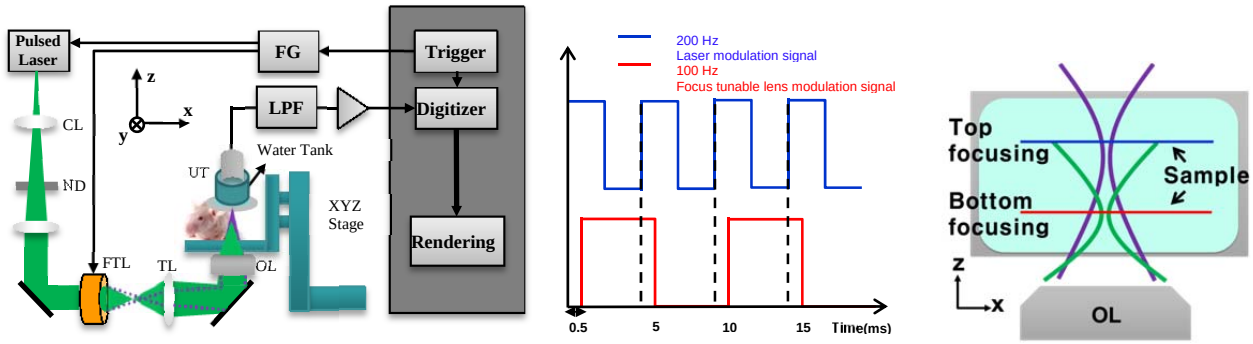

(a) (b) (c)

Figure 1. (a) Schematic diagram of the multi-depth PAM. (b) Timing diagrams to synchronize the laser pulse and the FTL. (c) Top and bottom illuminations by changing focal length.. FG, function generator; ND, neutral density filter; UT, ultrasonic transducer; LPF, low pass filter; OL, object lens; LNA, low noise amplifier, CL, convex lens; FTL, focus tunable lens; TL, tube lens;

On the detection side, the PA signals were detected by an ultrasonic transducer with the central frequency of 25 MHz and the focal length of 20 mm. The measured PA signals were amplified by a low noise amplifier and filtered unwanted high frequency noise by a low pass filter with 55 MHz cutoff frequency. We controlled the modulation current of the FTL by function generator (AFG3022B, Tektronix Co. Ltd.), and acquired the PA signals using a high speed digitizer (ATS9350, Alazartech Inc.) with 100 MS/sec sapling rate. Fig.1(b) shows the timing diagrams to synchronize the laser pulse and the FTL. The laser modulation signal from the channel 1 and the FTL modulation signal from channel 2 of a function generator are 200 Hz and 100 Hz, respectively. The FTL has an over damping activity and require additional setting time to follow the modulation signals. To synchronize two modulation signals, the FTL modulation signal was delayed 0.5 msec. The multi-depth PAM system had two-axial scanning translation stage to move a sample and to acquire lateral PA images. Fig. 1(c) shows the top and bottom laser beam illuminations on the sample as following the focal depth change of the FTL.

We put a tungsten wire of 10 μm thickness and moved the wire about 1.1 mm different depth position in the water tank. As changing the focal length of the FTL, we maximized the PA signal from the wire. As shown in Fig. 2(a), the axial resolution was maintained ~100 μm independently the depth position of the wire. The blue and red lines are top and bottom illumination, respectively. The focal length of the FTL was changed about 50 mm. The PA signal change was obtained as moving sample continuously and adjusting the focal length simultaneously. The envelopes of the PA signals were broadly flat and the axial imaging range was enhanced as shown in Fig. 2(b). The deviation of the maximum PA signals was about 26 % as 2.3 mm moving the wire sample.

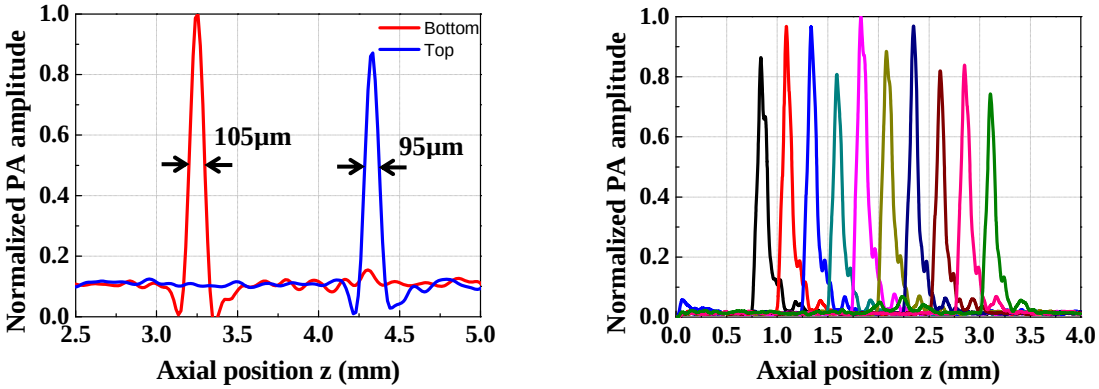

Figure 2. (a) PA amplitudes change with different depth positions of the tungsten wire sample and adjusting the focal length of the FTL. (b) PA amplitudes change as continuously moving the tungsten wire sample and adjusting the focal length of the FTL, simultaneously.

3. RESULTS

To measure the axial imaging range of multi-depth PAM system, we positioned a black human hair in diagonal direction of x and z-axis. We measured the maximum PA amplitudes of top and bottom by scanning with translation stage in Fig. 3(a). Each dot indicated maximum value of acquired PA signals during B-scan along x-axis. The red dots and the blue dots indicated that focal length was adjusted for illuminating the bottom and top layer, respectively. We merged the data sets of the acquired PA signals for the top and bottom focusing cases. The axial imaging range was about twice extended from 300 to 660 μm with objective lens (NA 0.4) as shown in Fig. 3(b). We measured imaging range using full width half maximum of PA amplitude. Figure 4(a), (b) show the volumetric PA images for the top and bottom focusing cases. The obtained PA signals were processed by low pass filtering and achieved the maximum intensity values. The PA images were achieved after image processing and volumetric rendering. Figure 4(c) shows the merged PA image of Fig. 4(a), (b). The axial imaging range was extended and the merged image shows the black hair over about 660 mm depth range.

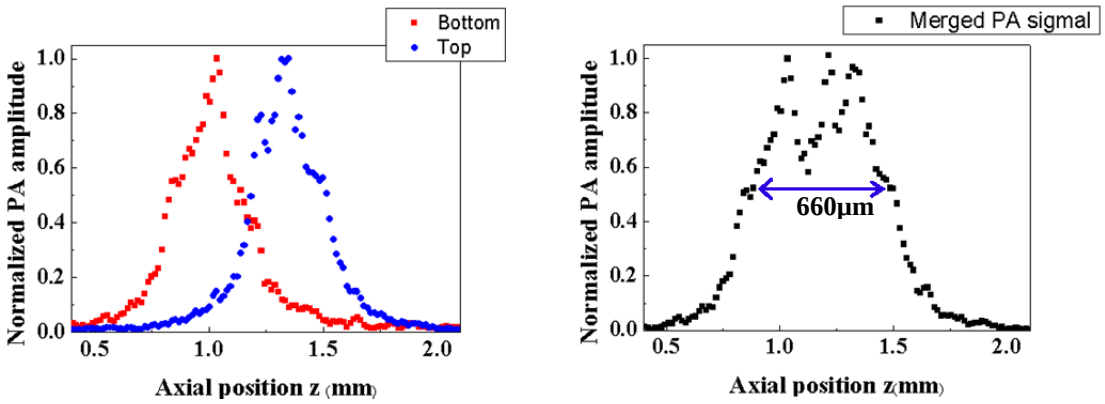

(a) (b)

Figure 3. (a) Maximum PA amplitudes for the top illuminating (blue dots) and the bottom illuminating (red dots). Each dot indicated maximum value of acquired PA signals during B-scan along x-axis. (b) By merging acquired PA signal, the extended axial imaging range was about 660 um (FWHM)

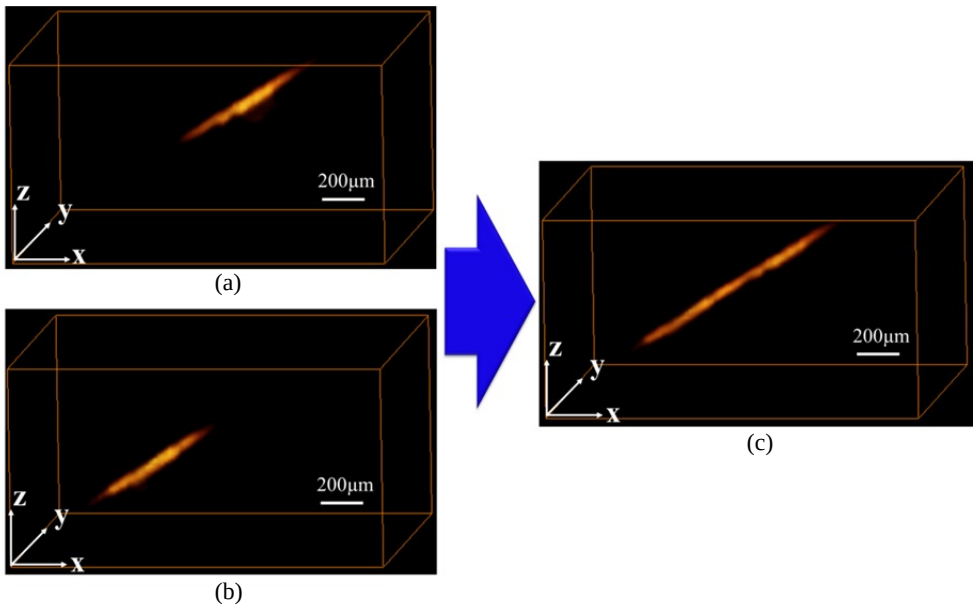

Figure 4. PA images of a black hair for top focusing (a), and bottom focusing (b), respectively. (c) The merged PA image from the top (a) and bottom (b) focusing

To demonstrate *in vivo* PA image based on the proposed multi-depth method, the vasculature of a living nude mouse ear (BALB/c Nude) was performed. The PA image of the mouse ear vasculature was obtained by the top layer focusing in Fig. 5(a). The left session vasculatures were positioned at the focal zone, but the right session vasculatures were out of the focal zone. In contrast as shown in Fig. 5(b), the PA image of the mouse ear vasculature was obtained by the bottom layer focusing. We could see some microvasculature in Fig. 5(b), which were not viewed in Fig. 4(a). We finally merged top and bottom PA images in Fig. 5(c) and enhanced the imaging range. The merged PA image is equivalent to the mouse ear photograph in Fig. 5(d). Likewise, we imaged more detail structure of the microvascular overall imaging plane as shown in Fig. 5(c). These PA images indicate the capability of providing many structural details of vasculature by using the multi-depth PAM system.

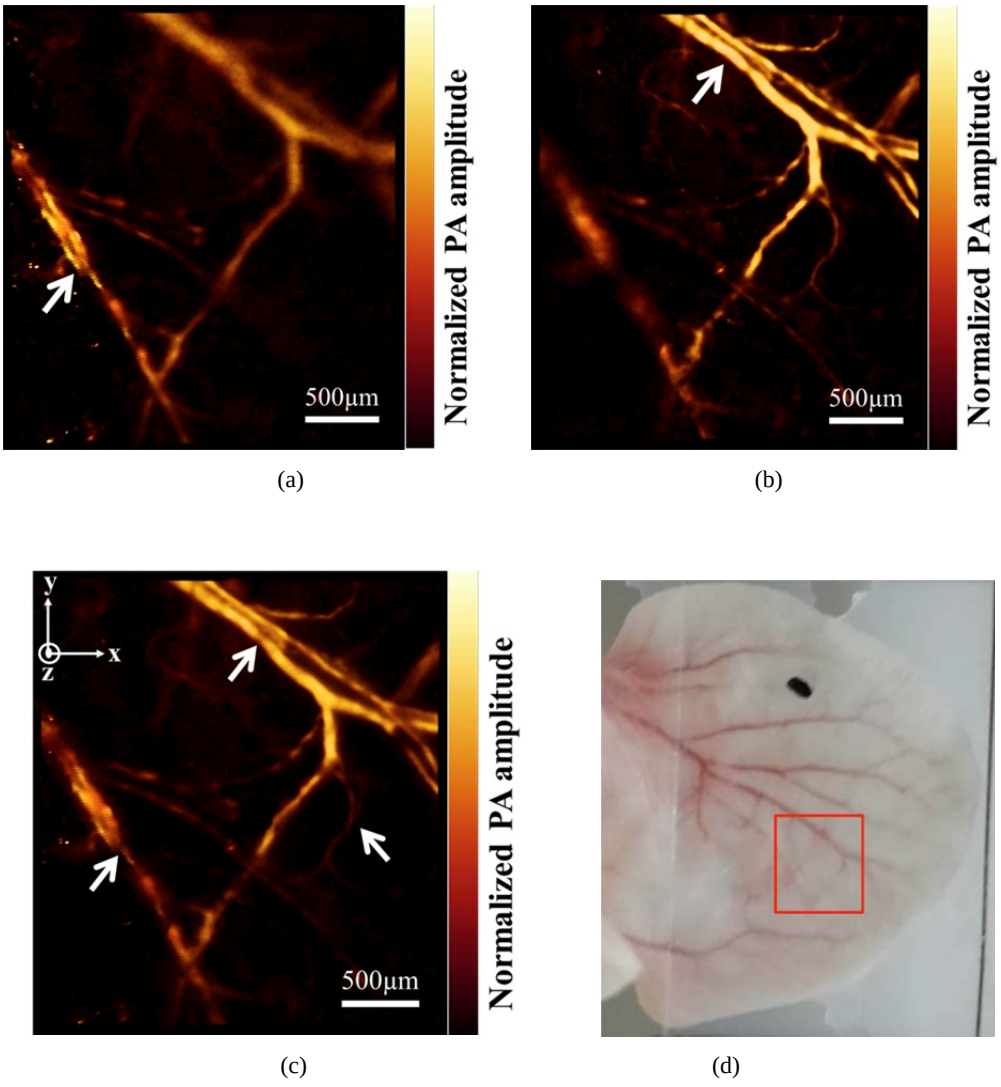

Figure 5. *In vivo* mouse ear PA image. (a) PA image with top layer focusing. (b) PA image with bottom layer focusing. (c) Merged PA image of the top (a) and bottom (b) focusing. (d) Photograph of the mouse ear.

4. DISCUSSION AND CONCLUSIONS

We demonstrated multi-depth PAM without mechanical movement. The focal length in the depth direction was electrically adjusted and the imaging range was twice extended from 300 to 660 μm with the NA 0.4 objective lens. The proposed multi-depth PAM system has the advantage of inertia-free fast focus scanning, which can avoid the motion artifacts. The FTL with fast response time (4.5msec) further shorten the total acquisition time. The multi-depth PAM system is more conductive to real-time PA imaging for a living biological tissue.

ACKNOWLEDGMENTS

This work was supported by the "Ultrashort Quantum Beam Facility Program" Project through a grant provided by GIST in 2015, the Industrial Strategic technology development program of the Ministry of Science, ICT & Future Planning, the industrial strategic technology development program (10047943) “Development of Micro-surgical Apparatus based on 3D Tomographic Operating Microscope” funded, and the new growth power equipment competitiveness reinforcement program (10047580) funded by the Ministry of Trade, industry & Energy (MI, Korea).

REFERENCES

[1] H. F. Zhang, K. Maslov, G. Stoica, and L. V. Wang, “Functional photoacoustic microscopy for high-resolution and noninvasive in vivo imaging,” Nat. Biotechnol. 24(7), 848–851 (2006).
[2] L. D. Wang et al., “Fast voice-coil scanning optical-resolution photoacoustic microscopy,” Opt. Lett. 36(2), 139–141 (2011).
[3] Z. L. Deng, X. Q. Yang, H. Gong, and Q. M. Luo, “Adaptive synthetic-aperture focusing technique for microvasculature imaging using photoacoustic microscopy,” Opt. Express 20(7), 7555–7563 (2012).
[4] Z. Y. Yang, J. H. Chen, J. J. Yao, R. Q. Lin, J. Meng, C. B. Liu, J. H. Yang, X. Li, L. Wang, and L. Song, “Multi-parametric quantitative microvascular imaging with optical-resolution photoacoustic microscopy in vivo,” Opt. Express 22(2), 1500–1511 (2014).
[5] J. M. Jabbour, M. A. Saldua, J. N. Bixler, and K. C. Maitland, “Confocal endomicroscopy: instrumentation and medical applications,” Ann. Biomed. Eng. 40(2), 378–397 (2012).
[6] J. Yao, K. I. Maslov, E. R. Puckett, K. J. Rowland, B. W. Warner, and L. V. Wang, “Double-illumination photoacoustic microscopy,” Opt. Lett. 37(4), 659–661 (2012).
[7] J. M. Jabbour, S. Cheng, B. H. Malik, R. Cuenca, J. A. Jo, J. Wright, Y. S. Cheng, and K. C. Maitland, “Fluorescence lifetime imaging and reflectance confocal microscopy for multiscale imaging of oral precancer,” J. Biomed. Opt. 18(4), 046012 (2013).
[8] A. A. Tanbakuchi, A. R. Rouse, J. A. Udovich, K. D. Hatch, and A. F. Gmitro, “Clinical confocal microlaparoscope for real-time in vivo optical biopsies,” J. Biomed. Opt. 14(4), 044030 (2009).
[9] K. B. Sung, C. Liang, M. Descour, T. Collier, M. Follen, and R. Richards-Kortum, “Fiber-optic confocal reflectance microscope with miniature objective for in vivo imaging of human tissues,” IEEE Trans. Biomed. Eng. 49(10), 1168–1172 (2002).
[10] I. Kurtz, R. Dwelle, and P. Katzka, "Rapid scanning fluorescence spectroscopy using an acousto-optic tunable filter," Rev. Sci. Instrum.58, 1996–2003 (1987).
[11] Optotune Application Note, “Optical focusing in microscopy with Optotune’s focus tunable lens EL-10-30”, Optotune, (2013)
[12] F. O. Fahrbach, F. F. Voigt, B. Schmid, F. Helmchen, and J. Huisken, “Rapid 3D light-sheet microscopy with a tunable lens,” Opt. Express 21(18), 21010–21026 (2013).